

# Electromagnetic Form Factors of Nucleons in a Relativistic Three-Quark Model

M. A. Ivanov\*, M. P. Locher, and V. E. Lyubovitskij\*\*

Paul Scherrer Institute, CH-5232 Villigen PSI, Switzerland

**Abstract.** We study electromagnetic form factors of nucleons within a relativistic three-quark model with a Gaussian shape for the nucleon-quark vertex. The allowed regions for two adjustable parameters, the range parameter  $\Lambda_N$  in the Gaussian and the constituent quark mass  $m_q$ , are obtained from fitting the data for magnetic moments and electromagnetic radii of nucleons. It is found that these observables, when calculated with  $m_q = 420$  MeV and  $\Lambda_N = 1.25$  GeV, agree very well with the experimental data. For these parameter values, however, our model underestimates the electromagnetic form factors of the nucleon at high momentum transfers for the calculated range  $0 \leq Q^2 \leq 1$  GeV<sup>2</sup>.

## 1 Introduction

Electromagnetic properties of nucleons are an important source of information on the internal structure of baryons. The success of the nonrelativistic quark model for the description of static characteristics (masses, magnetic moments, etc.) and the results from deep-inelastic lepton scattering are a clear indication for the three-quark structure of nucleons.

In view of the difficulties of describing the nucleon as a relativistic three-quark system rigorously, on the basis of QCD, many methods and models have been developed, which implement important aspects of QCD at least partially. We mention a few. Some approaches [1, 2] are formulated using classical hadronic degrees of freedom (colour singlets) without explicit reference to quarks and gluons. This holds in particular for chiral perturbation theory, which addresses low-energy scattering of hadrons [3]. In the Skyrmon model the baryon is considered to be a solitonic excitation of classical meson fields, which are described by an effective chiral Lagrangian, see ref. [4], for example. The electromagnetic radii and magnetic moments of nucleons as well

---

\* *Permanent address:* Bogoliubov Laboratory of Theoretical Physics, Joint Institute for Nuclear Research, 141980 Dubna, Russia

\*\* On leave of absence from: Bogoliubov Laboratory of Theoretical Physics, Joint Institute for Nuclear Research, 141980 Dubna, Russia. *Permanent address:* Department of Physics, Tomsk State University, 634050 Tomsk, Russia

as the behaviour of electromagnetic form factors up to  $1 \text{ GeV}^2$  are described in this way.

In the context of quark models the nonrelativistic approximation is problematic even for the constituent-quark picture at low energies since the effective masses and the intrinsic momenta have the same order of magnitude. Attempts to implement relativistic invariance for the description of the electromagnetic properties of the nucleon are the covariant constituent quark models by Konen and Weber [5] and Chung and Coester [6], which use light-front dynamics for the constituent quarks. In this framework the available data for  $0 \leq Q^2 \leq 1.5 \text{ GeV}^2$  [5] and  $0 \leq Q^2 \leq 6 \text{ GeV}^2$  [6] have been well described with two adjustable parameters (constituent quark mass and confinement scale).

For large momentum transfers,  $Q^2 \gg m_N^2$ , perturbative QCD predicts that the magnetic form factor behaves as  $G_M \sim 1/Q^4$  [7]. The use of QCD sum rules allows to extrapolate the electromagnetic form factors to low and moderate  $Q^2$  by incorporating local quark-hadron duality [8]. Recall that the calculation of hadronic form factors by sum rules in their original version [9] is restricted to intermediate momentum transfers and does not work in the infrared region due to power corrections  $1/Q^{2n}$ . Therefore, in order to calculate magnetic moments of nucleons QCD sum rules in the external-field approach have been introduced [10]. For a general method of calculating the nucleon magnetic form factors at small  $Q^2$  see ref. [11].

For applications at high energies the diquark model [12] has been proposed. In this model the proton is built from quarks and diquarks and the diquark is treated as a quasi-elementary particle. Fits to the data for  $Q^2 > 3 \text{ GeV}^2$  [13] with only a few parameters have been obtained.

A different line of attack uses both quark *and* hadronic degrees of freedom. Chiral potential models (see, for example, [14] and references therein) fall into this class. They use an effective confining potential for the quarks and a quark-pion interaction, which preserves chiral symmetry. Incorporating the lowest-order pionic correction, the magnetic moments of the nucleon octet have been calculated [14]. Alternative approaches [15–18] start from *effective Lagrangians*, which describe the transition of hadrons to their constituent quarks, combined with some assumptions on the behaviour of quarks at low energies and on the shape of the hadron-quark form factor. This approach is connected fairly directly to the difficult issues of hadronization and quark confinement in QCD.

In the present paper we extend the line of thought developed in refs. [19] and [20] using local hadron-quark or local hadron-quark-diquark vertices together with a confined quark propagator (no poles). It has been shown for these models that the electromagnetic form factors of nucleons tend to be somewhat above the data for  $Q^2 < 1 \text{ GeV}^2$ . This might be a hint that the assumption of a *local* coupling of baryons with their constituents is not quite adequate. Introducing a *nonlocal* hadron-quark vertex may be a good way of effectively introducing other degrees of freedom (mesonic cloud, soft gluons, etc.). The Nambu–Jona-Lasinio models (NJL) with separable interactions are examples of such attempts. Many successful applications of such models for low-energy pion physics exist (see, e.g., [15, 16] and references therein).

In refs. [21, 22] the Lagrangian formulation of the NJL model with separable interactions has been given both for mesons and (for the first time) for baryons. The gauging of nonlocal interactions has been done by using the time-ordering  $P$ -exponent.

The pion weak-decay constant, the two-photon decay width, as well as the form factor of the  $\gamma^* \pi^0 \rightarrow \gamma$  transition, the pion charge form factor, and the strong  $\pi NN$  form factor have been calculated and good agreement with the data has been achieved with only three parameters, the range parameters characterizing the sizes of mesons  $\Lambda_M$  and of baryons  $\Lambda_B$ , and the constituent quark mass  $m_q$ . In this paper we shall use the approach developed in refs. [21, 22] in order to calculate the electromagnetic form factors of nucleons. First, we slightly modify the gauging of the nonlocal quark-hadron vertex by using a path-independent definition for the derivative of the time-ordering  $P$ -exponent [23, 24]. Second, we derive Feynman rules for the diagrams that describe the electromagnetic nucleon form factors. For simplicity, we use a Gaussian shape for the nucleon-quark vertex. The permissible ranges for the two adjustable parameters, the Gaussian range  $\Lambda$  of the separable interaction and the constituent quark mass  $m_q$ , are obtained by fitting the experimental data of the magnetic moments and the electromagnetic radii.

## 2 Model

We start with a brief review of our approach. We consider the hadron as being a bound state of relativistic constituent quarks with masses  $m_q$  [21, 22]. The transition of hadrons into constituent quarks and *vice versa* is described by the corresponding interaction Lagrangian, and the momentum distribution of the constituents by an effective relativistic vertex function. Its shape is chosen to guarantee ultraviolet convergence. At the same time the vertex function is a phenomenological description of the long-distance QCD interactions between quarks and gluons.

The interaction Lagrangian of nucleons with quarks is written as

$$\begin{aligned} \mathcal{L}_N^{\text{int}}(x) &= \bar{N}(x) \int dy_1 \int dy_2 \int dy_3 \delta\left(x - \frac{y_1 + y_2 + y_3}{3}\right) F\left(\frac{1}{18} \sum_{i < j} (y_i - y_j)^2\right) \\ &\quad \times \{g_N^V J_N^V(y_1, y_2, y_3) + g_N^T J_N^T(y_1, y_2, y_3)\} + \text{h.c.} \\ &= \bar{N}(x) \int d\xi_1 \int d\xi_2 F(\xi_1^2 + \xi_2^2) \left\{ g_N^V J_N^V(x - 2\xi_1, x + \xi_1 - \sqrt{3}\xi_2, x + \xi_1 + \sqrt{3}\xi_2) \right. \\ &\quad \left. + g_N^T J_N^T(x - 2\xi_1, x + \xi_1 - \sqrt{3}\xi_2, x + \xi_1 + \sqrt{3}\xi_2) \right\} + \text{h.c.} \end{aligned} \quad (1)$$

with  $J_N^V$  and  $J_N^T$  being the vector and tensor currents, respectively. The currents are symmetric under permutation of any two quarks

$$J_N^V(y_1, y_2, y_3) = \bar{\tau} \gamma^\mu \gamma^5 q^{a_1}(y_1) q^{a_2}(y_2) \tau_2 \bar{\tau} C \gamma_\mu q^{a_3}(y_3) \varepsilon^{a_1 a_2 a_3}, \quad (2)$$

$$J_N^T(y_1, y_2, y_3) = \bar{\tau} \sigma^{\mu\nu} \gamma^5 q^{a_1}(y_1) q^{a_2}(y_2) \tau_2 \bar{\tau} C \sigma_{\mu\nu} q^{a_3}(y_3) \varepsilon^{a_1 a_2 a_3}. \quad (3)$$

The notation is as follows:  $\{a\}$  stands for the colour indices,  $\sigma^{\mu\nu} = (i/2)[\gamma^\mu, \gamma^\nu]$ , and  $C = \gamma^0 \gamma^2$  is the charge-conjugation matrix.

The notation for the spin-flavour structure of the nucleon currents is the same as in refs. [10, 25]. In particular, the proton quark currents in terms of isotopic  $u$  and  $d$  fields have the form

$$J_p^V = \gamma^\mu \gamma^5 d^a u^b C \gamma_\mu u^c \varepsilon^{abc}, \quad (4)$$

$$J_p^T = \sigma^{\mu\nu} \gamma^5 d^a u^b C \sigma_{\mu\nu} u^c \varepsilon^{abc}. \quad (5)$$

Both forms have been used separately in refs. [19, 20] for studying the electromagnetic and strong properties of baryons. It was shown that the tensor current (5) is more suitable for the description of the data, for which reason we shall also adopt it in the approach developed here.

The vertex form factor  $F(\xi_1^2 + \xi_2^2)$  characterizes the distribution of  $u$  and  $d$  quarks inside the nucleon. The choice of variables in the vertex function  $F(\xi_1^2 + \xi_2^2)$  implies the use of the centre-of-mass frame in which the coordinates of quarks are expressed as

$$y_1 = x - 2\xi_1, \quad y_2 = x + \xi_1 - \sqrt{3}\xi_2, \quad y_3 = x + \xi_1 + \sqrt{3}\xi_2, \quad (6)$$

where

$$\xi_1 = \frac{y_2 + y_3 - 2y_1}{6}, \quad \xi_2 = \frac{y_3 - y_2}{2\sqrt{3}}$$

are the Jacobi coordinates of the three-quark system.

The Fourier transform of the vertex form factor is defined as

$$F(\xi_1^2 + \xi_2^2) = \int \frac{d^4 k_1}{(2\pi)^4} \int \frac{d^4 k_2}{(2\pi)^4} \exp(-ik_1 \xi_1 - ik_2 \xi_2) F(k_1^2 + k_2^2).$$

To introduce the electromagnetic field into the nonlocal nucleon-quark Lagrangian (1), we shall use the time-ordering  $P$ -exponential [21, 22]. The interaction of quarks with the electromagnetic field is introduced by the standard minimal substitution.

Thus, we have the gauge-invariant interaction Lagrangian

$$\begin{aligned} \mathcal{L}_N^{\text{int,GI}}(x) = & g_N \bar{N}(x) \int dy_1 \int dy_2 \int dy_3 \delta\left(x - \frac{y_1 + y_2 + y_3}{3}\right) F\left(\frac{1}{18} \sum_{i < j} (y_i - y_j)^2\right) \\ & \times \Gamma_1 \vec{\tau} \exp\left(ieQ \int_x^{y_1} dz_\mu A^\mu\right) q^{a_1}(y_1) \exp\left(ieQ \int_x^{y_2} dz_\mu A^\mu\right) q^{a_2}(y_2) \\ & \times C \Gamma_2 \tau_2 \vec{\tau} \exp\left(ieQ \int_x^{y_3} dz_\mu A^\mu\right) q^{a_3}(y_3) \epsilon^{a_1 a_2 a_3} + \text{h.c.}, \end{aligned} \quad (7)$$

where  $\Gamma_1$  and  $\Gamma_2$  are spin matrices, and  $Q = \text{diag}(\frac{2}{3}, -\frac{1}{3}, -\frac{1}{3})$  is the charge matrix of quarks.

This interaction Lagrangian generates nonlocal vertices that couple nucleons, photons, and quarks. In general several diagrams contribute. For example, the electromagnetic form factors of nucleons are described by the standard triangle diagram (Fig. 1 a) and, additionally, by the bubble or contact diagrams (Fig. 1 b and Fig. 1 c).

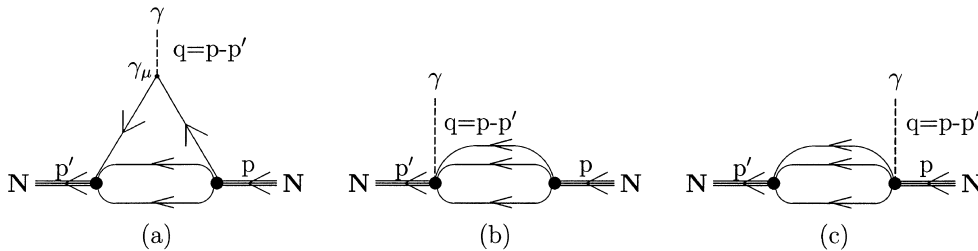


**Fig. 1.** Nucleon form factor. Triangle diagram (a), bubble diagrams (b) and (c)

At this stage the physical matrix elements describing the electromagnetic processes depend on the path which connects the lower and upper limits in the integral of the  $P$ -exponential. In the papers [21, 22] we used a straight line in our calculations. Here, we shall use a path-independent formalism, which is based on the path-independent definition [23] of the derivative of the line integral. This formalism has been used in ref. [24] for gauging nonlocal Lagrangians. We recall that the derivative of the line integral

$$I(x, y, P) \equiv \int_y^x dz_\mu A^\mu(z),$$

where  $P$  is the path taken from  $y$  to  $x$ , may be defined as [23]

$$\lim_{dx_\mu \rightarrow 0} dx_\mu \frac{\partial}{\partial x^\mu} I(x, y, P) = \lim_{dx_\mu \rightarrow 0} [I(x + dx, y, P') - I(x, y, P)]. \quad (8)$$

Here  $P'$  is obtained from the path  $P$  by adding the extension  $dx$  to the  $x$  end. Using the definition (8) leads to

$$\frac{\partial}{\partial x^\mu} I(x, y, p) = A_\mu(x). \quad (9)$$

This means that the derivative of the  $I(x, y, p)$  does not depend on the path used in the definition.

The method for deriving Feynman rules in the nonlocal chiral quark model with the electromagnetic  $P$ -exponential has been developed in ref. [24]. The crucial point is to calculate the expression

$$F(-\partial_x^2) e^{-ipx} I(x, y, p)$$

using Eq. (9).

It is readily seen that

$$F(-\partial_x^2) e^{-ipx} I(x, y, P) = e^{-ipx} F(-\mathcal{D}_x^2) I(x, y, P),$$

where  $\mathcal{D}_x^2 \equiv (\partial_x - ip)^2$ . Thus we need to calculate

$$F(-\mathcal{D}_x^2) I(x, y, P) = \sum_{n=0}^{\infty} (-)^n \frac{F^{(n)}(0)}{n!} \mathcal{D}_x^{2n} I(x, y, P).$$

One finds that

$$\mathcal{D}_x^2 I(x, y, P) = (\partial_x A(x)) - 2i(pA(x)) - p^2 I(x, y, P) \equiv L(A) - p^2 I(x, y, P),$$

where  $L(A) \equiv (\partial_x A(x)) - 2i(pA(x))$ . Then

$$(\mathcal{D}_x^2)^2 I(x, y, P) = (\mathcal{D}_x^2 - p^2) L(A) + (-p^2)^2 I(x, y, P),$$

$$(\mathcal{D}_x^2)^3 I(x, y, P) = ((\mathcal{D}_x^2)^2 - \mathcal{D}_x^2 p^2 + p^4) L(A) + (-p^2)^3 I(x, y, P),$$

$\vdots$

$$\begin{aligned} (\mathcal{D}_x^2)^n I(x, y, P) &= \sum_{k=0}^{n-1} (\mathcal{D}_x^2)^{n-1-k} (-p^2)^k L(A) + (-p^2)^n I(x, y, P) \\ &= n \int_0^1 dt [\mathcal{D}_x^2 t - p^2(1-t)]^{n-1} L(A) + (-p^2)^n I(x, y, P). \end{aligned}$$

Finally, this leads to

$$\begin{aligned} F(-\mathcal{D}_x^2)I(x, y, P) &= \int_0^1 dt F'[-\mathcal{D}_x^2 t + p^2(1-t)]L(A) + F(p^2)I(x, y, P) \\ &= \int dq A_\mu(q) \left\{ (q^\mu + 2p^\mu) e^{-iqx} \int_0^1 dt F'[(p+q)^2 t + p^2(1-t)] \right. \\ &\quad \left. + F(p^2) \int_y^x dz^\mu e^{-iqz} \right\}. \end{aligned}$$

We observe that the last term vanishes due to the delta function  $\delta(x-y)$  in the Lagrangian.

For baryons one has to calculate

$$F(-\partial_1^2 - \partial_2^2) e^{-ip_1 \xi_1 - ip_2 \xi_2} \int_y^{x+a_1 \xi_1 + a_2 \xi_2} dz^\mu A_\mu(z).$$

By analogy we get

$$\begin{aligned} &\int dq A_\mu(q) e^{-ip_1 \xi_1 - ip_2 \xi_2} \left\{ e^{-iq(x+a_1 \xi_1 + a_2 \xi_2)} [(-ia_1)(a_1 q^\mu + 2p_1^\mu)F_1 \right. \\ &\quad \left. + (-ia_2)(a_2 q^\mu + 2p_2^\mu)F_2] + F(p_1^2 + p_2^2) \int_y^{x+a_1 \xi_1 + a_2 \xi_2} dz^\mu e^{-iqz} \right\} \end{aligned}$$

with  $F_1$  and  $F_2$  being defined as

$$\begin{aligned} F_1 &= \int_0^1 dt F'[(p_2 + a_2 q)^2 + t(p_1 + a_1 q)^2 + (1-t)p_1^2], \\ F_2 &= \int_0^1 dt F'[p_1^2 + t(p_2 + a_2 q)^2 + (1-t)p_2^2]. \end{aligned} \quad (10)$$

With this preparation the Feynman rules for the  $\gamma NN$  vertex function may be derived. The details are given in Appendix A for the evaluation of the vertex in Fig. 2, which connects a nucleon, a photon, and three quarks, while Appendix B gives the connection to the nucleon mass operator of Fig. 3.

Now we turn to a discussion of the model aspects of our approach and the parameters involved. First, there is the vertex function in the Lagrangian (1). This is a free function except that it should make the Feynman diagrams ultraviolet finite, as we have mentioned before. In the papers [21, 22] we have found that the basic physical observables of pion low-energy physics depend only weakly on the choice of the vertex

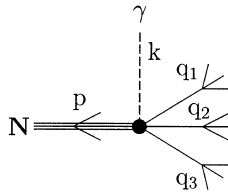


**Fig. 2.** Nucleon-photon three-quark vertex

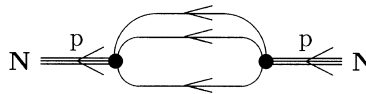


**Fig. 3.** Nucleon mass operator

functions considered. Therefore, we choose in this paper a Gaussian vertex function for simplicity. In Minkowski space we write

$$F(k_1^2 + k_2^2) = \exp\left(\frac{k_1^2 + k_2^2}{\Lambda_N^2}\right),$$

where  $\Lambda_N$  is the Gaussian range parameter which is related to the size of the nucleon.

The second input is the quark propagator. In the present paper we shall use the standard form, corresponding to a free fermionic field with mass  $m_q$ ,

$$\langle 0 | T(q(x)\bar{q}(y)) | 0 \rangle = \int \frac{d^4k}{(2\pi)^4} e^{-ik(x-y)} S_q(k), \quad S_q(k) = \frac{1}{m_q - \not{k}}. \quad (11)$$

Of course, the deficiency of such a choice is the lack of confinement. This could be corrected by changing the analytic properties of the propagator. We leave that to a future study. For the time being we shall avoid the appearance of unphysical imaginary parts in the Feynman diagrams by restricting the calculations to  $m_N < 3m_q$ .

Thus, there are two adjustable parameters in our model: the constituent quark mass  $m_q$  and the range parameter  $\Lambda_N$ . We shall determine them by fitting the electromagnetic properties of nucleons.

### 3 Nucleon Mass Operator and the $\gamma NN$ Vertex Function

Within the relativistic quark model described above we shall evaluate the magnetic moments, the charge radii, and the behaviour of the electric and magnetic form factors for  $0 \leq Q^2 \leq 1 \text{ GeV}^2$ .

It is convenient to separate the contributions from the triangle diagram (Fig. 1 a) and the bubble diagrams (Figs. 1 b and 1 c) as follows,

$$\Lambda_\mu(p, p') = \frac{q_\mu}{q^2} [\Sigma_N(p) - \Sigma_N(p')] + \Lambda_{\mu,\Delta}^\perp(p, p') + \Lambda_{\mu,\text{bubble}}^\perp(p, p'). \quad (12)$$

The functions  $\Lambda_{\mu,\Delta}^\perp(p, p')$  and  $\Lambda_{\mu,\text{bubble}}^\perp(p, p')$  are the modified triangle and bubble vertex functions, which are orthogonal to the photon momentum  $q^\mu \Lambda_\mu^\perp(p, p') = 0$ . Thus the Ward-Takahashi identity following from Eq. (12) reads

$$q^\mu \Lambda_\mu(p, p') = \Sigma_N(p) - \Sigma_N(p'). \quad (13)$$

In particular, if  $q = 0$  and both nucleons are on the mass shell, one finds

$$\Lambda_\mu(p, p) = \frac{\partial}{\partial p_\mu} \Sigma_N(p). \quad (14)$$

The expressions for the orthogonal parts of the vertex functions are

$$\begin{aligned} \Lambda_{\mu,\Delta}^\perp(p, p') &= 216(g_N^T)^2 \int \frac{d^4k}{(2\pi)^4} \int \frac{d^4k'}{(2\pi)^4} \\ &\times F(12[k^2 + k'^2 + kk']) F(12[k^2 + k'^2 + kk'] + 4q^2 - 12kq) \\ &\times [36QZ_\mu^\perp(k, p, p') \Pi_{PP}(k, k', p) + 36Q\gamma_5 Z_\mu^\perp(k, p, p') \gamma_5 \Pi_{SS}(k, k', p) \\ &+ \vec{\tau} Q \vec{\sigma}^{\alpha\beta} \gamma_5 Z_\mu^\perp(k, p, p') \sigma^{\rho\sigma} \gamma_5 \Pi_{TT}^{\alpha\beta, \rho\sigma}(k, k', p)] \end{aligned}$$

$$\begin{aligned}
\Lambda_{\mu, \text{bubble}}^{\perp}(p, p') &= 216(g_N^T)^2 \int \frac{d^4 k}{(2\pi)^4 i} \int \frac{d^4 k'}{(2\pi)^4 i} F(12[k^2 + kk' + k'^2]) k_{\mu}^{\perp} \\
&\times \frac{F(12[k^2 + k'^2 + kk'] + 4q^2 - 12kq) - F(12[k^2 + k'^2 + kk'])}{q^2 - 3kq} \\
&\times \left[ 36Q S_q \left( k + \frac{p}{3} \right) \Pi_{PP}(k, k', p) + 36Q \gamma_5 S_q \left( k + \frac{p}{3} \right) \gamma_5 \Pi_{SS}(k, k', p) \right. \\
&\left. + \bar{\tau} Q \bar{\tau} \sigma^{\alpha\beta} \gamma_5 S_q \left( k + \frac{p}{3} \right) \sigma^{\rho\sigma} \Pi_{TT}^{\alpha\beta, \rho\sigma}(k, k', p) \right] + (p \leftrightarrow p'),
\end{aligned}$$

where

$$\begin{aligned}
Z_{\mu}^{\perp} &= S_q \left( k + p' - \frac{2p}{3} \right) \gamma_{\mu}^{\perp} S_q \left( k + \frac{p}{3} \right), \quad Q = \text{diag}(\frac{2}{3}, -\frac{1}{3}), \quad \bar{\tau} Q \bar{\tau} = \text{diag}(0, 1), \\
\gamma_{\mu}^{\perp} &= \gamma_{\mu} - q_{\mu} \not{q} / q^2, \quad k_{\mu}^{\perp} = k_{\mu} - q_{\mu} k \cdot q / q^2 \quad (\gamma^{\perp} \cdot q = 0 \quad \text{and} \quad k^{\perp} \cdot q = 0),
\end{aligned}$$

and

$$\begin{aligned}
\Pi_{PP}(k, k', p) &= \text{tr} \left[ \gamma_5 S_q \left( k' + \frac{p}{3} \right) \gamma_5 S_q \left( k + k' - \frac{p}{3} \right) \right], \\
\Pi_{SS}(k, k', p) &= \text{tr} \left[ S_q \left( k' + \frac{p}{3} \right) S_q \left( k + k' - \frac{p}{3} \right) \right], \\
\Pi_{TT}^{\alpha\beta, \rho\sigma}(k, k', p) &= \text{tr} \left[ \sigma^{\alpha\beta} S_q \left( k' + \frac{p}{3} \right) \sigma^{\rho\sigma} S_q \left( k + k' - \frac{p}{3} \right) \right].
\end{aligned}$$

The nucleon-three-quark coupling  $g_N^T$  is calculated from the *compositeness condition* (see ref. [17]), which means that the renormalization constant of the nucleon wave function is equal to zero,  $Z_N = 1 - \Sigma'_N(m_N) = 0$ , with  $\Sigma_N$  being the nucleon mass operator

$$\begin{aligned}
\Sigma_N(p) &= 216(g_N^T)^2 \int \frac{d^4 k}{(2\pi)^4 i} \int \frac{d^4 k'}{(2\pi)^4 i} F^2(12[k^2 + k'^2 + kk']) \\
&\times \left[ 12 S_q \left( k + \frac{p}{3} \right) \Pi_{PP}(k, k', p) + 12 \gamma_5 S_q \left( k + \frac{p}{3} \right) \gamma_5 \Pi_{SS}(k, k', p) \right. \\
&\left. + \sigma^{\alpha\beta} \gamma_5 S_q \left( k + \frac{p}{3} \right) \sigma^{\rho\sigma} \gamma_5 \Pi_{TT}^{\alpha\beta, \rho\sigma}(k, k', p) \right]. \tag{15}
\end{aligned}$$

The calculation of the electromagnetic vertex functions and of the nucleon mass operators is given in Appendix B.

#### 4 Numerical Results and Discussion

We start with a summary of well-known definitions for the electromagnetic properties of the nucleon. The vertex functions in terms of Dirac  $F_D^{(p,n)}$  and Pauli  $F_P^{(p,n)}$  form



factors are

$$M_\mu = \bar{N}^i(p') \Lambda_\mu^{ij}(p, p') N^j(p),$$

$$\Lambda_\mu^{ij}(p, p') = \gamma_\mu F_D^{ij}(q^2) - \frac{i}{2m_N} \sigma_{\mu\nu} q^\nu F_P^{ij}(q^2), \quad (16)$$

where  $N(p)$  and  $N(p')$  are the spinors corresponding to initial and final nucleon states with momentum  $p$  and  $p'$ , respectively, and

$$\bar{N} = (\bar{p} \quad \bar{n}), \quad N = \begin{pmatrix} p \\ n \end{pmatrix},$$

$$F_D = \begin{pmatrix} F_D^p & 0 \\ 0 & F_D^n \end{pmatrix}, \quad F_P = \begin{pmatrix} F_P^p & 0 \\ 0 & F_P^n \end{pmatrix}. \quad (17)$$

The electric and magnetic (Sachs) form factors are obtained from

– electric form factors

$$G_E^{(p,n)}(q^2) = F_P^{(p,n)}(q^2) + \frac{q^2}{4m_N^2} F_D^{(p,n)}(q^2),$$

– magnetic form factors

$$G_M^{(p,n)}(q^2) = F_P^{(p,n)}(q^2) + F_D^{(p,n)}(q^2).$$

At zero recoil,  $q^2 = 0$ , these form factors satisfy the following normalization conditions

$$G_E^p(0) = 1, \quad G_E^n(0) = 0,$$

$$G_M^p(0) = \mu_p, \quad G_M^n(0) = \mu_n,$$

where  $\mu_p$  and  $\mu_n$  are the magnetic moments of the proton and the neutron, respectively.

The charge radii of the nucleons are given by

$$\langle r^2 \rangle_E^p = \frac{6}{G_E^p(0)} \left. \frac{dG_E^p(q^2)}{dq^2} \right|_{q^2=0} = \left[ F_D^{p'}(0) + \frac{\mu_p - 1}{4m_N^2} \right], \quad (18)$$

$$\langle r^2 \rangle_E^n = 6 \left. \frac{dG_E^n(q^2)}{dq^2} \right|_{q^2=0} = 6 \left[ F_D^{n'}(0) + \frac{\mu_n}{4m_N^2} \right], \quad (19)$$

$$\langle r^2 \rangle_M^N = \frac{6}{G_M^N(0)} \left. \frac{dG_M^N(q^2)}{dq^2} \right|_{q^2=0} = \frac{6}{\mu_N} [F_D^{N'}(0) + F_P^{N'}(0)]. \quad (20)$$

We shall work in the limit of isospin invariance where the masses of  $u$  and  $d$  quarks are equal,  $m_u = m_d = m_q$ . In a first step we set the parameters of our model  $m_q$  and  $\Lambda_N$  to the well-measured static properties of the nucleons, to the magnetic moments, and to the charge radii [26, 27]. In a second step we shall explore the constraints from the shape of the nucleon electromagnetic form factors for the range  $Q^2 \leq 1 \text{ GeV}^2$ .

In Table 1 the results for the static properties are given for various sets of parameters  $m_q$  and  $\Lambda_N$ . As was mentioned above, the constituent mass  $m_q$  is chosen higher than one-third of the nucleon mass ( $m_q > m_N/3$ ) to avoid an imaginary part in the Feynman

**Table 1.** Static nucleon properties

$m_q, \Lambda_N$ in GeV	$\mu_p$	$\mu_n$	$ \mu_p/\mu_n $	$r_E^p$ (fm)	$\langle r^2 \rangle_E^n$ (fm <sup>2</sup> )	$r_M^p$ (fm)	$r_M^n$ (fm)
0.315, 2.40	2.78	-1.77	1.57	0.91	-0.171	0.84	0.85
0.320, 2.25	2.79	-1.79	1.56	0.88	-0.169	0.80	0.81
0.325, 2.12	2.81	-1.81	1.55	0.88	-0.166	0.79	0.80
0.330, 2.00	2.82	-1.82	1.55	0.88	-0.162	0.79	0.80
0.335, 1.90	2.82	-1.84	1.53	0.88	-0.159	0.79	0.80
0.340, 1.80	2.82	-1.85	1.52	0.89	-0.155	0.80	0.80
0.350, 1.70	2.82	-1.85	1.52	0.89	-0.152	0.80	0.80
0.360, 1.60	2.83	-1.86	1.52	0.89	-0.148	0.81	0.81
0.370, 1.50	2.82	-1.87	1.51	0.90	-0.144	0.82	0.82
0.380, 1.40	2.82	-1.87	1.51	0.91	-0.139	0.83	0.83
0.390, 1.35	2.81	-1.87	1.50	0.92	-0.137	0.84	0.84
0.400, 1.30	2.81	-1.87	1.50	0.92	-0.135	0.84	0.84
0.410, 1.30	2.79	-1.86	1.50	0.91	-0.134	0.83	0.83
0.420, 1.25	2.79	-1.86	1.50	0.92	-0.132	0.84	0.84
0.430, 1.25	2.77	-1.86	1.49	0.91	-0.132	0.83	0.83
0.440, 1.25	2.76	-1.85	1.49	0.90	-0.131	0.82	0.82
0.450, 1.25	2.76	-1.85	1.49	0.89	-0.131	0.81	0.81
0.460, 1.20	2.75	-1.85	1.49	0.90	-0.129	0.82	0.82
0.470, 1.20	2.74	-1.84	1.49	0.89	-0.129	0.82	0.81
0.480, 1.15	2.74	-1.84	1.49	0.90	-0.127	0.83	0.82
0.490, 1.15	2.73	-1.84	1.48	0.90	-0.127	0.82	0.82
0.500, 1.15	2.73	-1.84	1.48	0.89	-0.127	0.82	0.81
Exp.	2.79	-1.91	1.46	$0.86 \pm 0.01$	$-0.119 \pm 0.004$	$0.86 \pm 0.06$	$0.88 \pm 0.07$

diagrams. Its value is varied in the region from 315 MeV to 500 MeV. One of the important constraints is the ratio of magnetic moments of proton and neutron  $R = |\mu_p/\mu_n|$ , which is measured with high accuracy to be  $R = 1.46$ . Historically, the first success in describing this value was achieved in a naive nonrelativistic  $SU(6)$  quark model. The value  $R_{SU(6)} = 1.5$  [28] is already close to experiment. It is seen from Table 1 that in our approach this value varies in the range  $R = 1.50$ – $1.57$ , when the quark mass is smaller than 400 MeV, and starts to be less than 1.5 for  $m_q > 400$  MeV. The electric neutron radius squared,  $\langle r^2 \rangle_E^n$ , is also sensitive to the choice of the quark mass. In this case as well, the best agreement with experiment is achieved for  $m_q > 400$  MeV. As can be seen from Eq. (19) the neutron charge radius is a combination of the neutron Dirac form factor  $F_D^{n'}(0)$  and the ratio  $3\mu_n/2m_N^2$ . Using the experimental value for the neutron magnetic moment the last term almost reproduces the experimental value for  $\langle r^2 \rangle_E^n$ . This means that the contribution coming from  $F_D^{n'}(0)$  should be negligibly small ( $F_D^{n'}(0) \simeq 0.008$ ). One can see from Table 2 that this value, disregarding its sign, is indeed small for  $m_q > 400$  MeV what confirms a consistent trend for the value of  $m_q$ . Therefore we consider  $m_q = 400$  MeV to be a lower bound for the constituent quark mass in our model. Our results for magnetic moments get worse for  $m_q > 500$  MeV (see Table 1). The value of 500 MeV may therefore be considered an approximate upper bound for  $m_q$ .

**Table 2.** Contribution of Dirac form factor to nucleon radii (cf. Eqs. (19)–(21))

$m_q, \Lambda_N$ in GeV	$F_D^{p'}(0)$ in $\text{GeV}^{-2}$	$F_D^{n'}(0)$ in $\text{GeV}^{-2}$
0.315, 2.40	3.04	−0.229
0.320, 2.25	2.80	−0.215
0.330, 2.00	2.80	−0.176
0.340, 1.80	2.89	−0.138
0.350, 1.70	2.87	−0.125
0.360, 1.60	2.87	−0.115
0.370, 1.50	2.95	−0.085
0.380, 1.40	3.02	−0.073
0.390, 1.35	3.10	−0.055
0.400, 1.30	3.10	−0.047
0.410, 1.30	3.04	−0.045
0.420, 1.25	3.11	−0.037
Exp.	2.66	0.008

As will be seen below the behaviour of the nucleon electromagnetic form factors is sensitive to the choice of the constituent quark mass. Increasing the constituent quark mass above 500 MeV and reducing the parameter  $\Lambda_N$  below 1.15 GeV improves agreement with the static nucleon properties. However, the form factors at  $Q^2 = 1 \text{ GeV}^2$  are then definitely getting too low. Thus the value  $m_q = 500 \text{ MeV}$  is an upper limit in our model also from the point of view of the form factors.

The electric radius of the proton and the magnetic radii of protons and neutrons depend fairly weakly on the parameters  $m_q$  and  $\Lambda_N$ . The theoretical values for the neutron electric radius squared show the right trend as well, despite the small size of this quantity. In Table 3 the best fit of the nucleon static properties for  $m_q = 420 \text{ MeV}$  and

**Table 3.** Static properties compared to theoretical approaches

Approach	$\mu_p$	$\mu_n$	$r_E^p$ , fm	$\langle r^2 \rangle_E^n$ , fm <sup>2</sup>	$r_M^p$ , fm	$r_M^n$ , fm
Our	2.79	−1.86	0.92	−0.132	0.84	0.84
Ioffe [10]	2.96	−1.93				
Balitsky [29]	2.80	−1.95				
Meißner [4]	2.77	−1.84	0.97	−0.25	0.94	0.94
Aznauryan [30]	2.811	−1.848	0.811	−0.094	0.825	0.781
Weber [5]	2.80	−1.73	0.83	−0.023	0.78	0.79
Isgur [31]	2.79	−1.86				
Baric [14]	2.73	−1.975	0.85			
Dorokhov [32]	2.20	−1.47	0.831	0		
De Grand [33]	1.90	−1.27	0.728	0		
Exp.	2.79	−1.91	$0.86 \pm 0.01$	$-0.119 \pm 0.004$	$0.86 \pm 0.06$	$0.88 \pm 0.07$

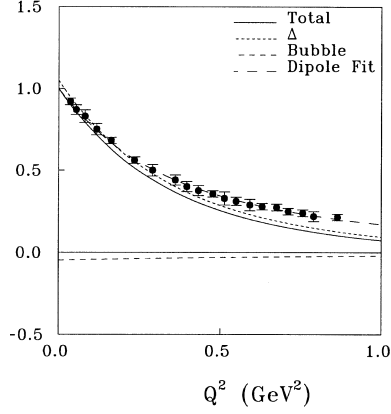


**Fig. 4.** Magnetic form factor of proton

$\Lambda_N = 1.25$  GeV is compared to other theoretical approaches such as QCD sum rules [10, 29], the nonlinear chiral model of ref. [4], the relativistic invariant quark model in the light-front formalism of ref. [30], the relativistic constituent quark model [5], the nonrelativistic quark model of ref. [31], the relativistic quark model with chiral symmetry of ref. [14]), the nonrelativistic quark model with QCD-vacuum-induced quark interactions of ref. [32] and the MIT bag model [33].

The shape of the electromagnetic nucleon form factors in the region  $0 \leq Q^2 \leq 1$  GeV<sup>2</sup> for the same optimal values of the parameters,  $m_q = 420$  MeV and  $\Lambda_N = 1.25$  GeV, is shown in Figs. 4–7. The normalized magnetic form factors  $G_M^N(Q^2)/G_M^N(0)$  are plotted in Fig. 4 and Fig. 5.

The short dashed line corresponds to the contribution of the triangle vertex function  $\Lambda_{\mu,\Delta}^\perp(p, p')$  whereas the medium-long dashed line gives the contribution of the bubble or contact term  $\Lambda_{\mu,\text{bubble}}^\perp(p, p')$ . This contribution is roughly constant and not large. It matters, however, for the details of the fitting procedure. The total contribution is marked by the solid line. The long-dashed line is the dipole approximation, which fits the data taken from ref. [34] quite well. The electric form factors of the proton and the neutron are shown in Figs. 6 and 7, respectively. The figures show that the form factors  $F_E^p, F_M^p$ , and  $F_M^n$  fall off faster than the experimental data in the range  $0 \leq Q^2 \leq 1$  GeV<sup>2</sup>.

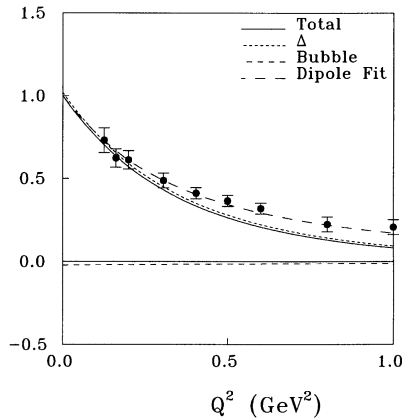


**Fig. 5.** Magnetic form factor of neutron

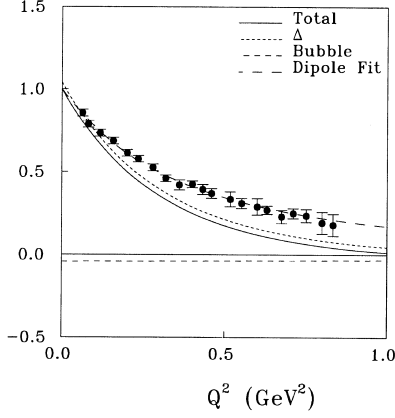


**Fig. 6.** Electric form factor of proton

To illustrate the deviation from the data we show in Fig. 8 the three form factors normalized to the dipole fit of ref. [34]. For the electric form factor of the neutron the calculation agrees within the large experimental error bars. Within the constraints given by the static properties the momentum dependence of the form factors cannot be improved in our model, what in part may be due to our Gaussian parametrization of the nucleon-quark vertex.

## 5 Conclusion

The electromagnetic form factors of nucleons have been calculated within a relativistic three-quark model with Gaussian shape for the nucleon-quark vertex, and standard (non-confined) quark propagators. Gauge invariance of the nonlocal hadron-quark interaction has been implemented by the path-independent definition for the derivative of the time-ordering  $P$ -exponent. The allowed region for the two adjustable parameters, the range parameter  $\Lambda_N$  appearing in the Gaussian and the constituent quark mass  $m_q$ , has been obtained by fitting the data for the magnetic moments and the electromagnetic radii of the nucleons. We find that their values calculated with  $m_q = 420 \text{ MeV}$  and  $\Lambda_N = 1.25 \text{ GeV}$  agree very well with the experimental data while the form factors  $F_E^p$ ,

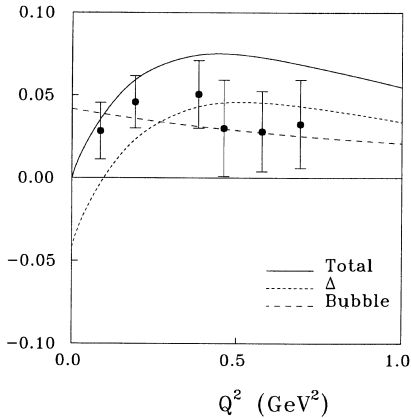


**Fig. 7.** Electric form factor of neutron

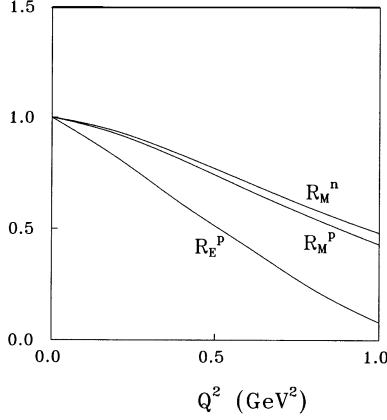


**Fig. 8.** Nucleon form factors scaled by the dipole fit:  $R_E^p$  electric form factor of proton,  $R_M^p$  magnetic form factor of proton,  $R_M^n$  magnetic form factor of neutron

$F_M^p$ , and  $F_M^n$  are too low at high momentum transfers in the calculated range, a problem which in part is presumably related to the Gaussian ansatz for the quark-nucleon vertex function. We plan to extend the calculation to the axial form factors and weak-decay matrix elements of baryons.

*Acknowledgements.* We would like to thank P. Kroll, R. Rosenfelder, J. Bolz, H. Kamada, and H.-Q. Zheng for useful discussions. This work was supported in part by the INTAS Grant 94-739, by the Russian Fund of Fundamental Research (RFFR) under contracts 94-02-03463-a, 96-02-17435-a and the State Committee of the Russian Federation for Education (project N 95-0-6.3-67, Grand Center at St.-Petersburg State University).

## Appendix A. Feynman Rules for Nonlocal Electromagnetic Vertices

We illustrate how to obtain a nonlocal vertex that couples a nucleon, a photon, and three quarks (see Fig. 2). The analogous nonlocal vertices with mesons were introduced in ref. [24]. Let  $p$  denote the momentum of the outgoing baryon,  $k$  the momentum of the outgoing photon, and  $q_1, q_2, q_3$  the momenta of incoming quarks, respectively. We start from the gauge-invariant Lagrangian describing the interaction of nucleons with quarks, Eq. (7). The vertex function  $\Gamma^\mu(q_1 q_2 q_3 p k)$  corresponding to Fig. 2 is

$$i(2\pi)^4 \delta^{(4)}\left(p - k - \sum_{i=1}^3 q_i\right) \Gamma_{a_1 a_2 a_3}^\mu(q_1 q_2 q_3 p k) = \int dx_1 \cdots \int dx_5 \exp\left[i\left(\sum_{i=1}^3 q_i x_i - p x_4 - k x_5\right)\right] \times R_{a_1 a_2 a_3}^\mu(x_1 \cdots x_5), \quad (\text{A.1})$$

where the function  $R_{a_1 a_2 a_3}^\mu(x_1 \cdots x_5)$  is given by

$$R_{a_1 a_2 a_3}^\mu(x_1 \cdots x_5) = \frac{\delta^5\left[\int dx \mathcal{L}_N^{\text{int,GI}}(x)\right]}{\delta A_\mu(x_5) \delta \bar{N}(x_4) \delta q^{a_1}(x_1) \cdots \delta q^{a_3}(x_3)} \Big|_{A_\mu=0} \\ = e g_N e^{a_1 a_2 a_3}(\Gamma_1) \times (C \Gamma_2) F \left[ \frac{1}{18} \sum_{i < j}^3 (x_i - x_j)^2 \right] \delta\left(x_4 - \frac{1}{3} \sum_{i=1}^3 x_i\right) \\ \times \left[ (\vec{\tau} Q) \times (\tau_2 \vec{\tau}) \int_{x_4}^{x_1} dz^\mu + \vec{\tau} \times (Q \tau_2 \vec{\tau}) \int_{x_4}^{x_2} dz^\mu + \vec{\tau} \times (\tau_2 \vec{\tau} Q) \int_{x_4}^{x_3} dz^\mu \right] \delta(x_5 - z). \quad (\text{A.2})$$

We define a typical integral as

$$I_{\text{typ}}^\mu = \int dx_1 \cdots \int dx_5 \exp \left[ i \left( \sum_{i=1}^3 q_i x_i - p x_4 - k x_5 \right) \right] F \left[ \frac{1}{18} \sum_{i < j}^3 (x_i - x_j)^2 \right] \delta \left( x_4 - \frac{1}{3} \sum_{i=1}^3 x_i \right) \int_{x_4}^{x_1} dz^\mu \delta(x_5 - z),$$

which may be written as

$$\begin{aligned} I_{\text{typ}}^\mu &= 6\sqrt{3} \int dx \int d\xi_1 \int d\xi_2 F(\xi_1^2 + \xi_2^2) \exp \left[ ix \left( \sum_{i=1}^3 q_i - p \right) \right] \\ &\quad \times \exp[\xi_1(-2q_1 + q_2 + q_3) + i\xi_2\sqrt{3}(q_3 - q_2)] \int_x^{x-2\xi_1} dz^\mu \exp[-ikz]. \end{aligned} \quad (\text{A.3})$$

Using the identity

$$\begin{aligned} \int d\xi_1 \int d\xi_2 f(\xi_1, \xi_2) F(\xi_1^2 + \xi_2^2) &= \int d\xi_1 \int d\xi_2 f(\xi_1, \xi_2) F(-\partial_{\xi_1}^2 - \partial_{\xi_2}^2) \delta(\xi_1) \delta(\xi_2) \\ &= \int d\xi_1 \int d\xi_2 \delta(\xi_1) \delta(\xi_2) F(-\partial_{\xi_1}^2 - \partial_{\xi_2}^2) f(\xi_1, \xi_2) \end{aligned}$$

one finds

$$\begin{aligned} I_{\text{typ}}^\mu &= 6\sqrt{3} \int dx \int d\xi_1 \int d\xi_2 \delta(\xi_1) \delta(\xi_2) \exp \left[ ix \left( \sum_{i=1}^3 q_i - p \right) \right] F(-\partial_{\xi_1}^2 - \partial_{\xi_2}^2) \\ &\quad \times \left\{ \exp[i\xi_1(-2q_1 + q_2 + q_3) + i\xi_2\sqrt{3}(q_3 - q_2)] \int_x^{x-2\xi_1} dz^\mu \exp[-ikz] \right\}. \end{aligned}$$

Finally, using the transformations described in Sect. 2 we obtain

$$\begin{aligned} I_{\text{typ}}^\mu &= i(2\pi)^4 \delta^{(4)} \left( p - k - \sum_{i=1}^3 q_i \right) 24\sqrt{3}(q_2 + q_3 - 2q_1 + k)^\mu M(q_1, q_2, q_3, k), \\ M(q_1, q_2, q_3, k) &= \frac{F[\Delta(q_1, q_2, q_3, k)] - F[\Delta(q_1, q_2, q_3, 0)]}{\Delta(q_1, q_2, q_3, k) - \Delta(q_1, q_2, q_3, 0)}, \\ \Delta(q_1, q_2, q_3, k) &= 4 \left[ \sum_{i=1}^3 q_i^2 + k^2 - \sum_{i < j}^3 q_i q_j + k(q_2 + q_3 - 2q_1) \right]. \end{aligned} \quad (\text{A.4})$$

Employing the result for the typical integral (A.4) in Eq. (A.1) we can write the vertex function  $\Gamma_{a_1 a_2 a_3}^\mu(q_1 q_2 q_3 p k)$  as

$$\begin{aligned} \Gamma_{a_1 a_2 a_3}^\mu(q_1 q_2 q_3 p k) &= 24\sqrt{3} e g_N \varepsilon^{a_1 a_2 a_3} (\Gamma_1) \times (C \Gamma_2) [\vec{\tau} Q \times (\tau_2 \vec{\tau})(q_2 + q_3 - 2q_1 + k)^\mu M(q_1, q_2, q_3, k) \\ &\quad + \vec{\tau} \times (Q \tau_2 \vec{\tau})(q_3 + q_1 - 2q_2 + k)^\mu M(q_2, q_3, q_1, k) \\ &\quad + \vec{\tau} \times (\tau_2 \vec{\tau} Q)(q_1 + q_2 - 2q_3 + k)^\mu M(q_3, q_1, q_2, k)]. \end{aligned} \quad (\text{A.5})$$

## Appendix B. The Nucleon Mass Operator and the $\gamma NN$ Vertex

To demonstrate the calculation of an electromagnetic vertex and nucleon mass operator we consider the two generic integrals

$$\begin{aligned} I_1(p_E^2, p_E'^2, Q^2) &= \int \frac{d^4 k_E}{\pi^2} \int \frac{d^4 k_E'}{\pi^2} \prod_{i=1}^4 \frac{1}{m_q^2 + P_{iE}^2} \\ &\quad \times F(-12[k_E^2 + k_E'^2 + k_E k_E']) F(-12[k_E^2 + k_E'^2 + k_E k_E'] - 4Q^2 + 12k_E Q), \end{aligned}$$

$$I_2(p_E^2, p_E'^2, Q^2) = \int \frac{d^4 k_E}{\pi^2} \int \frac{d^4 k_E'}{\pi^2} \int_0^1 dt \prod_{i=1}^3 \frac{1}{m_q^2 + P_{iE}^2} F(-12[k_E^2 + k_E'^2 + k_E k_E']) \\ \times F'(-12[k_E^2 + k_E'^2 + k_E k_E'] - t[4Q^2 - 12k_E Q]) \quad (\text{B.1})$$

with the Euclidean momenta  $P_{iE}$  being related to nucleon momenta  $p_E, p_E'$  by

$$P_{1E} = k_E + p_E/3, \quad P_{2E} = k_E' + p_E/3, \quad P_{3E} = k_E + k_E' - p_E/3, \\ P_{4E} = k_E + p_E' - 2p_E/3, \quad Q = p_E - p_E'.$$

The first integral arises in the calculation of the triangle vertex function or the derivative of the nucleon mass operator (in this case  $p_E = p_E'$ ). The second integral arises in the calculation of the bubble vertex functions.

Using the Feynman parametrization

$$\frac{1}{A} = \int_0^\infty d\alpha \exp(-\alpha A)$$

and integrating over  $k_E$  and  $k_E'$  one finds for on-mass-shell nucleons

$$I_1(-m_N^2, -m_N^2, Q^2) = \int_0^\infty \dots \int_0^\infty \frac{d\alpha_1 \dots d\alpha_4}{\Delta_1^2} \exp \left[ -\frac{3Q^2}{\Delta_1} (2 + \alpha_{12})(1 + 2\alpha_{34}) \right] \\ \times \exp \left[ -\frac{4m_N^2}{3\Delta_1} ((1 + \alpha_{34})(\alpha_1 - \alpha_2)^2 + (1 + \alpha_1)(\alpha_{34} - \alpha_2)^2 + (1 + \alpha_2)(\alpha_{34} - \alpha_1)^2) \right] \\ \times \exp \left[ -12 \left( m_q^2 - \frac{m_N^2}{9} \right) \sum_{i=1}^4 \alpha_i \right] \\ I_2(-m_N^2, -m_N^2, Q^2) = 12 \int_0^1 dt \int_0^\infty \dots \int_0^\infty \frac{d\alpha_1 \dots d\alpha_3}{\Delta_2^2} \exp \left[ -\frac{3Q^2 t}{\Delta_2} (2 + \alpha_{12})(2 + 2\alpha_3 - t) \right] \\ \times \exp \left[ -\frac{4m_N^2}{3\Delta_2} ((1 + \alpha_3)(\alpha_1 - \alpha_2)^2 + (1 + \alpha_1)(\alpha_3 - \alpha_2)^2 + (1 + \alpha_2)(\alpha_3 - \alpha_1)^2) \right] \\ \times \exp \left[ -12 \left( m_q^2 - \frac{m_N^2}{9} \right) \sum_{i=1}^3 \alpha_i \right].$$

Introducing the notation  $\alpha_{ij} = \alpha_i + \alpha_j$  we have

$$\Delta_1 = 3 + 2 \sum_{i=1}^4 \alpha_i + \alpha_{12}\alpha_{34} + \alpha_1\alpha_2, \quad \Delta_2 = 3 + 2 \sum_{i=1}^3 \alpha_i + \sum_{i<j}^3 \alpha_i\alpha_j.$$

Making a change of variables

$$\alpha_1 = xs, \quad \alpha_2 = x(1-s), \quad \alpha_3 = yt, \quad \alpha_4 = y(1-t) \quad \text{in integral } I_1(-m_N^2, -m_N^2, Q^2), \\ \alpha_1 = xs, \quad \alpha_2 = x(1-s), \quad \alpha_3 = y, \quad \quad \quad \text{in integral } I_2(-m_N^2, -m_N^2, Q^2),$$

one finds

$$I_1(-m_N^2, -m_N^2, Q^2) = \int_0^\infty dx \int_0^\infty dy \int_0^1 ds \frac{xy}{\Delta^2} \exp \left[ -\frac{3Q^2}{\Delta} (2+x)(1+2y) \right] \\ \times \exp \left[ -\frac{4m_N^2}{3\Delta} ((1+y)(1-2s)^2 x^2 + (1+xs)(y-x(1-s))^2 \right. \\ \left. + (1+x(1-s))(y-xs)^2) \right] \exp \left[ -12(x+y) \left( m_q^2 - \frac{m_N^2}{9} \right) \right], \quad (\text{B.2})$$



$$\begin{aligned}
I_2(-m_N^2, -m_N^2, Q^2) = 12 \int_0^\infty dx \int_0^\infty dy \int_0^1 ds \int_0^1 dt \frac{x}{\Delta^2} \exp \left[ -\frac{3Q^2 t}{\Delta} (2+x)(2+2y-t) \right] \\
\times \exp \left[ -\frac{4m_N^2}{3\Delta} ((1+y)(1-2s)^2 x^2 + (1+xs)(y-x(1-s))^2 \right. \\
\left. + (1+x(1-s))(y-xs)^2) \right] \exp \left[ -12(x+y) \left( m_q^2 - \frac{m_N^2}{9} \right) \right], \quad (\text{B.3})
\end{aligned}$$

where  $\Delta = 3 + 2(x+y) + x^2 s(1-s) + xy$ .

## References

1. Cahill, R. T., Roberts, C. D.: Phys. Rev. **D32**, 2419 (1985)
2. Andrianov, A. A., Andrianov, V. A., Novozhilov, V. Yu., Novozhilov, Yu. V.: Lett. Math. Phys. **11**, 217 (1986); Phys. Lett. **B186**, 401 (1987)
3. Gasser, J., Leutwyler, H.: Ann. Phys. (NY) **158**, 142 (1984)
4. Meissner, U.-G., Kaiser, N., Weigel, H., Schechter, J.: Phys. Rev. **D39**, 1956 (1989)
5. Konen, W., Weber, H. J.: Phys. Rev. **D41**, 2201 (1990)
6. Chung, P. L., Coester, F.: Phys. Rev. **D44**, 229 (1991)
7. Lepage, G. P., Brodsky, S. J.: Phys. Rev. **D22**, 2157 (1980)
8. Radyushkin, A. V.: Acta Phys. Pol. **B15**, 403 (1984); Nesterenko, V. A., Radyushkin, A. V.: Phys. Lett. **B128**, 439 (1984)
9. Shifman, M. A., Vainshtein, A. I., Zakharov, V. I.: Nucl. Phys. **B147**, 385 (1979)
10. Ioffe, B. L., Smilga, A. V.: Nucl. Phys. **B232**, 109 (1984)
11. Belyaev, V. M., Kogan, Ya. I.: Preprint ITEP-29 (1984); Int. J. Mod. Phys. **A8**, 153 (1993)
12. Kroll, P., Schürmann, M., Schweiger, W.: Z. Phys. **338**, 339 (1991)
13. Andivahis, L., et al.: Nucl. Phys. **A553**, 713 (1993)
14. Baric, N., Dash, B. K.: Phys. Rev. **D34**, 2803 (1986); Tegen, R., Brockmann, R., Weise, W.: Z. Phys. **A307**, 339 (1982)
15. Goldman, T., Haymaker, R. W.: Phys. Rev. **D24**, 724 (1981)
16. Ito, H., Buck, W. W., Gross, F.: Phys. Rev. **C45**, 1918 (1992); Bowler, R. D., Birse, M. C.: Nucl. Phys. **A582**, 655 (1995)
17. Efimov, G. V., Ivanov, M. A.: The Quark Confinement Model of Hadrons. Bristol, Philadelphia: IOP Publishing 1993
18. Efimov, G. V., Nedelko, S. N.: Phys. Rev. **D51**, 176 (1995)
19. Efimov, G. V., Ivanov, M. A., Lyubovitskij, V. E.: Few-Body Systems **6**, 17 (1989)
20. Efimov, G. V., Ivanov, M. A., Lyubovitskij, V. E.: Z. Phys. **C47**, 583 (1990)
21. Anikin, I. V., et al.: Phys. Atom. Nucl. **57**, 1082 (1994)
22. Anikin, I. V., et al.: Z. Phys. **C65**, 681 (1995)
23. Mandelstam, S.: Ann. Phys. (NY) **19**, 1 (1962)
24. Terning, J.: Phys. Rev. **D44**, 887 (1991)
25. Chung, Y.: Nucl. Phys. **B197**, 55 (1982)
26. Review of Particle Properties (Particle Data Group): Phys. Rev. **D50**, 1173 (1994)
27. Dumbrajs, O., et al.: Nucl. Phys. **B216**, 216 (1983)
28. Greenberg, O. W.: Ann. Rev. Nucl. Part. Sci. **28**, 327 (1978)
29. Balitsky, I. I., Yung, A. V.: Phys. Lett. **B129**, 328 (1983)
30. Aznauryan, I. G., Bagdasryan, A. S., Ter-Isaakyan, N. L.: Phys. Lett. **B112**, 393 (1982)
31. Isgur, N., Karl, G.: Phys. Rev. **D18**, 4187 (1978); **D19**, 2653 (1979); **D20**, 1191 (1979); Hayne, C., Isgur, N.: Phys. Rev. **D25**, 1944 (1982); Capstick, S., Isgur, N.: Phys. Rev. **D34**, 2809 (1986)
32. Dorokhov, A. E., Kochelev, N. I., Zubov, Yu. A.: Sov. J. Nucl. Phys. **D23**, 522 (1992)
33. de Grand, T., Jaffe, R. L., Johnson, K., Kiskis, J.: Phys. Rev. **D12**, 2060 (1975)
34. Höhler, G., et al.: Nucl. Phys. **B114**, 505 (1976).

Received April 10, 1996; revised June 20, 1996; accepted for publication July 19, 1996